THE JOURNAL OF COMPARATIVE NEUROLOGY 385:427–440 (1997)

Interneurons in the Stratum Lucidum of the Rat Hippocampus: An Anatomical and Electrophysiological Characterization

NELSON SPRUSTON,[1,2] JOACHIM LÜBKE,[3] AND MICHAEL FROTSCHER[3]*
[1]Max-Planck-Institut für medizinische Forschung, Abteilung Zellphysiologie, D-69120 Heidelberg, Germany
[2]Department of Neurobiology and Physiology, Institute for Neuroscience, Northwestern University, Evanston, IL 60208-3520
[3]Anatomisches Institut, Albert-Ludwigs-Universität Freiburg, D-79001 Freiburg, Germany

ABSTRACT

The anatomical and electrophysiological properties of neurons in the stratum lucidum of the CA3 subfield of the hippocampus were examined by using patch-pipette recordings combined with biocytin staining. This method facilitated the analysis of the morphological features and passive and active properties of a recently described class of spiny neurons in the stratum lucidum, as well as aspiny neurons in this region. Some, but not all, synaptic inputs of both types of neurons were found to arise from the mossy fiber system. The axons of spiny neurons in the stratum lucidum were heavily collateralized, terminating primarily in the stratum lucidum and stratum radiatum of CA3, and to a lesser extent in the stratum pyramidale and stratum oriens. Only a few axonal projections were found that extended beyond the CA3 region into CA1 and the hilus. Aspiny neurons fell into two classes: those projecting axons to the stratum lucidum and stratum radiatum of CA3 and those with axon terminations mainly in the stratum pyramidale and stratum oriens. The electrophysiological properties of spiny and aspiny neurons in the stratum lucidum were similar, but on average, the aspiny neurons had significantly higher maximal firing rates and narrower action potential half-widths. The results demonstrate that a diverse population of neurons exists in the region of mossy fiber termination in area CA3. These neurons may be involved in local-circuit feedback, or feed-forward systems controlling the flow of information through the hippocampus. J. Comp. Neurol. 385:427–440, 1997.

Indexing terms: hippocampal interneuron; local circuit; passive membrane properties; patch-clamp; intracellular staining

The hippocampal formation (including the entorhinal cortex, the hippocampus proper, and the dentate gyrus) is believed to play a critical role in the formation of memories (Zola-Morgan and Squire, 1993) and the encoding of spatial location (Wilson and McNaughton, 1993). Knowledge of the different types of neurons in these regions, as well as their physiological properties and synaptic connections, is an important step toward understanding how the hippocampal formation carries out these functions. Specifically, biologically realistic neural networks modeled after the hippocampus require precise knowledge about the properties of the individual neuronal elements and the connections between them (Berger et al., 1994; Treves and Rolls, 1994).

The synaptic connections between the principal excitatory neurons of the hippocampus are well established (e.g., Frotscher, 1988; Amaral, 1993), as are the basic physiological properties of these neurons (Storm, 1987; Madison and Nicoll, 1984; Fricke and Prince, 1984; Spigelman et al., 1992; Spruston and Johnston, 1992; Staley et al., 1992). However, characterization of other cell types in the hippocampus is more difficult because within a given region many different cell types exist, making it essential to combine staining and light microscopic identification with physiological recording (see, for example, Misgeld and Frotscher, 1986; Scharfman, 1992; Buhl et al., 1994). Recently, a previously undescribed, spiny, nonpyramidal

Grant sponsor: Alexander von Humboldt Foundation; Grant sponsor: the von Helmholtz-Programm of the BMBF; Grant sponsor: the Leibniz Programm of the Deutsche Forschungsgemeinschaft; Grant number: Fr 620/1-6.

*Correspondence to: Michael Frotscher, Anatomisches Institut, Albert-Ludwigs-Universität Freiburg, P.O. Box 111, D-79001 Freiburg, Germany. E-mail: frotsch@sun2.ruf.uni-freiburg.de

Received 2 August 1996; Revised 10 March 1997; Accepted 21 March 1997

class of neurons was discovered in the stratum lucidum region of the hippocampus (Gulyás et al., 1992; Soriano and Frotscher, 1993a; Frotscher et al., 1994). These neurons are few in number and lie horizontal to the pyramidal layer of the CA3 region. It has been shown that the spiny stratum lucidum cells are extremely vulnerable to ischemia and may, therefore, play an important role in early pathological changes of the hippocampal formation (Freund and Maglóczky, 1993; Hsu and Buzsáki, 1993). Here, we take advantage of the ability to patch clamp visually identified neurons in hippocampal slices to characterize the physiological and morphological properties of horizontal neurons in the stratum lucidum. Use of the whole-cell patch-clamp technique facilitated determination of the physiological properties in the absence of a somatic leak, and also provided filling of the same neurons with biocytin, thus allowing morphological examination of these cells, including analysis of their axonal projections and synaptic contacts at the light and electron microscopic level.

MATERIALS AND METHODS

Patch-pipette recordings and biocytin filling

Brains were removed from 13- to 28-day-old Wistar rats killed by decapitation. Transverse hippocampal slices (300–400 μm) were cut in ice-cold physiological saline by using a Vibratome (FTB Vibracut, Heidelberg, Germany). Slices were then incubated at 32–35°C for 30–60 minutes, and subsequently at room temperature. Patch-clamp recordings were made under visual control by using infrared, differential-interference contrast (IR-DIC), video microscopy (Stuart et al., 1993), using an upright microscope (Axioskop FS, Zeiss, Oberkochen, Germany) with a ×40 water immersion objective (numerical aperture 0.75, 1.9 mm working distance), equipped with an infrared filter (RG-9, Schott, Melsungen, Germany), and a Newvicon camera (C2400, Hamamatsu, Tokyo, Japan).

Patch pipettes were pulled from borosilicate glass tubing (Hilgenberg, Malsfeld, Germany; 2.0 mm outer diameter, 0.5 mm wall thickness), and had resistances of 3–10 MΩ when filled with internal pipette solution (see below). Cells were approached while positive pressure was applied to the inside of the patch pipette. The pressure was released when a dimple was observed on the somatic membrane, and gentle suction, combined with hyperpolarization of the patch pipette, resulted in the formation of high resistance seals (>10 GΩ), in most cases. Seals were formed in the continuous single electrode voltage-clamp (SEVC) mode of an Axoclamp 2B amplifier (Axon Instruments, Foster City, CA). After breaking the patch membrane to obtain a whole-cell recording, the amplifier was switched to the bridge voltage-recording mode. The bridge balance was monitored occasionally throughout the experiment; series resistances (Rs) varied between 5 and 50 MΩ in different recordings. Patch-pipette recordings were performed either at room temperature (22–24°C) or at 34–37°C. Only the physiological data obtained at 34–37°C are reported.

Solutions and drugs

Physiological extracellular solution used for bath perfusion contained 125 mM NaCl, 25 mM $NaHCO_3$, 25 mM glucose, 2.5 mM KCl, 1.25 mM NaH_2PO_4, 2 mM $CaCl_2$, 1 mM $MgCl_2$, and was bubbled with a 95% O_2, 5% CO_2 gas mixture. In most experiments, 10 μM 6-cyano-7-nitroquinoxaline-2,3-dione (CNQX, Tocris), 50 μM D-2-amino-5-phosphonopentanoic acid (D-AP5, Tocris), and 10 μM bicuculline methiodide (BCC, Sigma, München, Germany) were included in the extracellular solution to block spontaneous synaptic activity. The internal pipette solution contained 130 mM K-gluconate, 20 mM KCl, 10 mM ethylene glycol bis (2-aminoethylether) N,N,N',N'-tetraacetic acid (EGTA), 10 mM HEPES, 2 mM $MgCl_2$, 2 mM adenosine 5'-triphosphate (ATP, di-sodium salt), and 5 mg/ml biocytin, pH was adjusted to 7.3 with KOH. All chemicals were obtained from Merck (Darmstadt, Germany) or Sigma (München, Germany).

Data acquisition and analysis

Voltage recordings were filtered at 3–10 kHz and were acquired on-line at sample rates of 10–20 kHz by using a VME-bus computer system (Motorola, Tempe, AZ). Data analysis was performed by using programs written for the same computer and Igor (Wavemetrics, Lake Oswego, OR) on a Macintosh Power PC computer. All statistical analyses were performed by using single factor analysis of variance with Tukey's multiple comparisons. Differences were regarded as statistically significant at the $P < 0.05$ level.

Determination of "passive" membrane properties

The input resistance (R_N) and membrane time constant (τ_m) were estimated from voltage responses to current injections (500–1,000 milliseconds long) as large as ±150 pA, and as small as ±5 pA. Both the peak and the steady-state (end of pulse) voltage responses were plotted versus current amplitude for each cell. R_N was determined from the slope of the steady-state responses in a linear region around, and including, the origin. τ_m was estimated from the slowest time constant (τ_0) of exponential fits to the voltage transients in the linear region of the V-I plot. Transients were not used for determination of τ_0 if there were other indications of nonlinearity, such as large differences in the τ_0 values from the on and off transients, or large differences in the τ_0 values of larger current injections compared with the smallest hyperpolarizing response (see Spruston and Johnston, 1992, for a description of the quantitative criteria used). Furthermore, transients were rejected if the peak-voltage response differed from the steady-state response at the end of the pulse by more than 20%, thus resulting in the rejection of noisy responses or those displaying considerable sag (Purpura et al., 1968). In some cells, these criteria were not met for any of the voltage transients collected. As a result, the n value for τ_0 is lower than for the other measurements, and is therefore reported separately, in Table 1. In cases where some sag was evident, transients were fit to the peak of the response, without constraining the baseline to be the same as the steady-state voltage at the end of the current pulse. These criteria provided a functional definition of the term "passive membrane properties," but, as was the case for the principal cell types of the hippocampus (Spruston and Johnston, 1992), voltage transients were not passive in the strict sense; small changes in membrane potential about rest resulted in different values of R_N and τ_0 in the same cell, suggesting that responses are in part determined by voltage-sensitive ion channels that are open at, or very near, the resting membrane potential. The values of R_N and τ_0 reported here are intended to serve as a characteriza-

TABLE 1. Physiological Properties of Hippocampal Stratum Lucidum Interneurons and CA3 Pyramidal Neurons[1]

Cell type	No. of cells[2]	Resting potential (mV)	R_N (MΩ)	τ_m (milliseconds)	Sag ratio	Maximum firing rate (spikes/second)	Spike width (milliseconds)	Fast ahp (mV)	Slow ahp (mV)
spiny s.l.	8 (8)	−59 ± 2	341 ± 69	42 ± 6	0.81 ± 0.04	75 ± 10	0.80 ± 0.07	−15.1 ± 1.6	−4.6 ± 2.0
		−69, −50	21, 782	19, 64	0.62, 0.96	35, 131	0.55, 1.09	−10.7, 6.2	−22.7, −8.6
aspiny s.l.	9 (7)	−61 ± 2	284 ± 60	28 ± 2	0.90 ± 0.02	115 ± 11	0.53 ± 0.07	−15.0 ± 2.2	−6.6 ± 1.3
		−67, −50	136, 720	21, 41	0.83, 0.97	75, 181	0.29, 1.05	−23.0, −6.3	−11.2, 1.8
CA3	3 (3)	−71 ± 4	193 ± 14	65 ± 8	0.94 ± 0.02	40 ± 12	0.71 ± 0.04	−5.4 ± 0.4	−7.7 ± 1.9
		−67, −50	171, 226	53, 85	0.89, 0.98	22, 69	0.66, 0.80	−6.2, −4.6	−11.8, −3.9

[1]For each parameter, mean ± SEM and range (low, high) are indicated.
[2]The n for τ_m is indicated in parentheses. See Materials and Methods for explanation.

tion of the properties of these neurons under physiological conditions (i.e., no attempt was made to linearize the membrane by blocking voltage-gated channels).

Determination of action potential firing properties

The maximal action potential firing rate was determined by using current injections (1–2 seconds long) of +100 to +900 pA. The slow afterhyperpolarization (slow ahp) was measured as the most negative potential (with respect to the resting membrane potential) after the train of the maximal-rate action potentials. Action potential half-width and fast afterhyperpolarization (fast ahp) were determined from the first spike in response to current injection just above threshold. Action potential amplitude and fast ahp were determined with respect to the spike threshold level.

Morphological analysis

Neurons were filled with biocytin, contained in the patch pipette, at a concentration of 5 mg/ml. Recordings were maintained for 15–60 minutes before pulling off the electrode. During electrode withdrawal, the amplifier was switched back to SEVC mode, and seal resistance was continuously monitored with a test pulse. Care was taken to form an outside-out patch to avoid creating a somatic leak through which the biocytin could escape. Thereafter, slices were immediately removed from the slice chamber and fixed with a 0.1 M phosphate-buffered solution (PB) containing 1% paraformaldehyde and 1% glutaraldehyde (pH 7.4). The inclusion of glutaraldehyde facilitated subsequent electron microscopic examination.

Fixed slices were rinsed several times in 0.1 M PB and then treated in H_2O_2 (3% in 0.1 M PB) for 15–30 minutes to eliminate endogenous peroxidase activity. Slices were then rinsed several times again with 0.1 M PB, followed by incubation in an ascending series of dimethylsulfoxide (DMSO, Merck; 5%, 10%, 20%, and 40% in 0.1 M PB; 20 minutes each) and further rinsing in 0.1 M PB. Thereafter, slices were incubated overnight at 4°C in an avidin-biotin horseradish peroxidase-complex solution prepared according to the manufacturer's protocol (Vector Laboratories, Burlingame, CA; diluted 1:200). After rinsing in 0.1 M PB, the slices were reacted in diaminobenzidine (DAB, Sigma Grade II). They were first preincubated for 20 minutes in the dark at 4°C in 0.025% DAB containing 0.002% NiH_4SO_4 and 0.0015% $CoCl_2$, and then reacted in a fresh DAB solution containing 0.002% H_2O_2 until the neuron stained by a dark brown reaction product was observed. After the DAB reaction, slices were rinsed in 0.1 M PB and distilled water, and then postfixed for 15–60 minutes in 0.5% OsO_4 dissolved in 0.1 M PB. They were then rinsed again in 0.1 M PB and distilled water, dehydrated in an ascending series of ethanol, and finally flat-embedded in Durcopan (Fluka, Chemie AG, Buchs, Switzerland). Labeled cells were photographed and reconstructed with the aid of a camera lucida. Serial ultrathin sections (silver interference color) were cut, stained with uranyl acetate and Reynold's lead citrate, and examined with a Zeiss EM 10 electron microscope (Zeiss, Oberkochen, Germany). Although the use of IR-DIC videomicroscopy to patch-clamp neurons near the surface facilitated routine filling and recording from neurons in stratum lucidum that would have been much more unlikely using "blind" recording, one of the disadvantages was that the ultrastructural features viewed at the level of the electron microscope were somewhat compromised, presumably due to damage caused during slicing of the live tissue (Frotscher et al., 1981). Nevertheless, the ultrastructure was sufficient to identify structures such as spines, presynaptic terminals, postsynaptic densities, and synaptic vesicles, thus permitting ultrastructural characterization of the properties of synaptic contacts to and from these neurons.

All protocols used in the present study were approved by the institutional committee for animal care.

RESULTS

Morphological identification of different cell types in stratum lucidum

Neurons in the stratum lucidum region of the hippocampal slice were visualized and patch-clamped using IR-DIC video microscopy (see Materials and Methods). Typically, only one or two neurons with their cell bodies in stratum lucidum could be visualized in the top 50–100 μm of each slice. In most cases the cell bodies of these neurons were oriented perpendicular to the layer of CA3 pyramidal neurons. Whereas all neurons located in stratum lucidum appeared similar in the living slice, closer examination of their morphology after biocytin staining revealed at least two populations: spiny neurons (14 of 38 neurons filled) and aspiny neurons (24 of 38 neurons). By using the presence or absence of spines as a criterion for cell classification, we followed previous descriptions of neurons in the stratum lucidum (Gulyás et al., 1992; Soriano and Frotscher, 1993a). A neuron was classified as spiny when at least a few spines were found on each of its dendrites (see Discussion).

Dendritic arborizations of spiny neurons

Two examples of spiny neurons in stratum lucidum are shown in Figure 1. These neurons were of bipolar morphology, with the cell body giving rise to 2–5 dendrites oriented

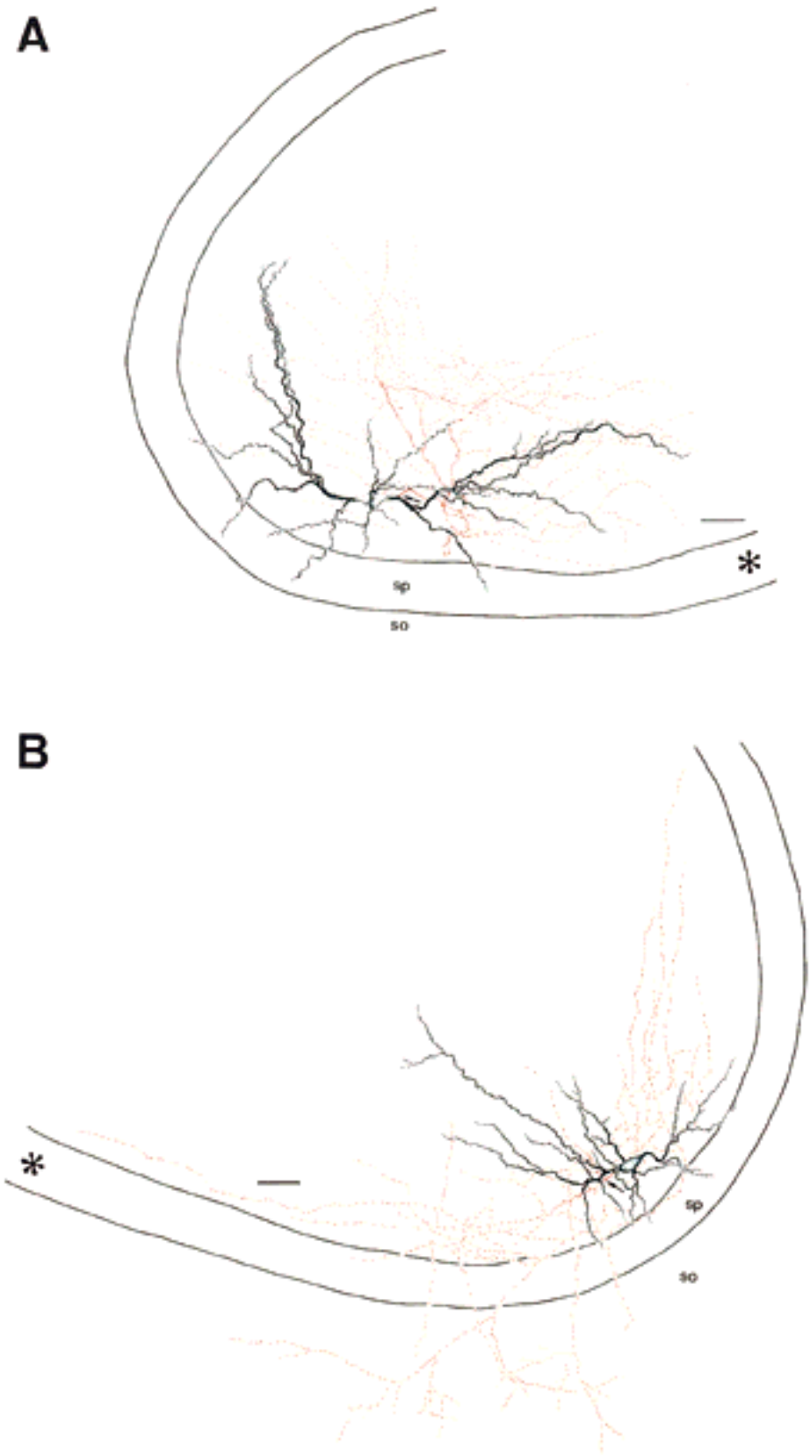

Fig. 1. **A,B:** Dendritic trees and axonal arborizations of two spiny neurons in stratum lucidum, intracellularly filled with biocytin. This figure demonstrates the position of the cell bodies in stratum lucidum, the extent of the dendritic arborization (black), and the extent of the axonal arborization (red). The small arrows point to the axon origin. Asterisks indicate hippocampal region CA3c. sp, stratum pyramidale; so, stratum oriens. Scale bars = 50 μm.

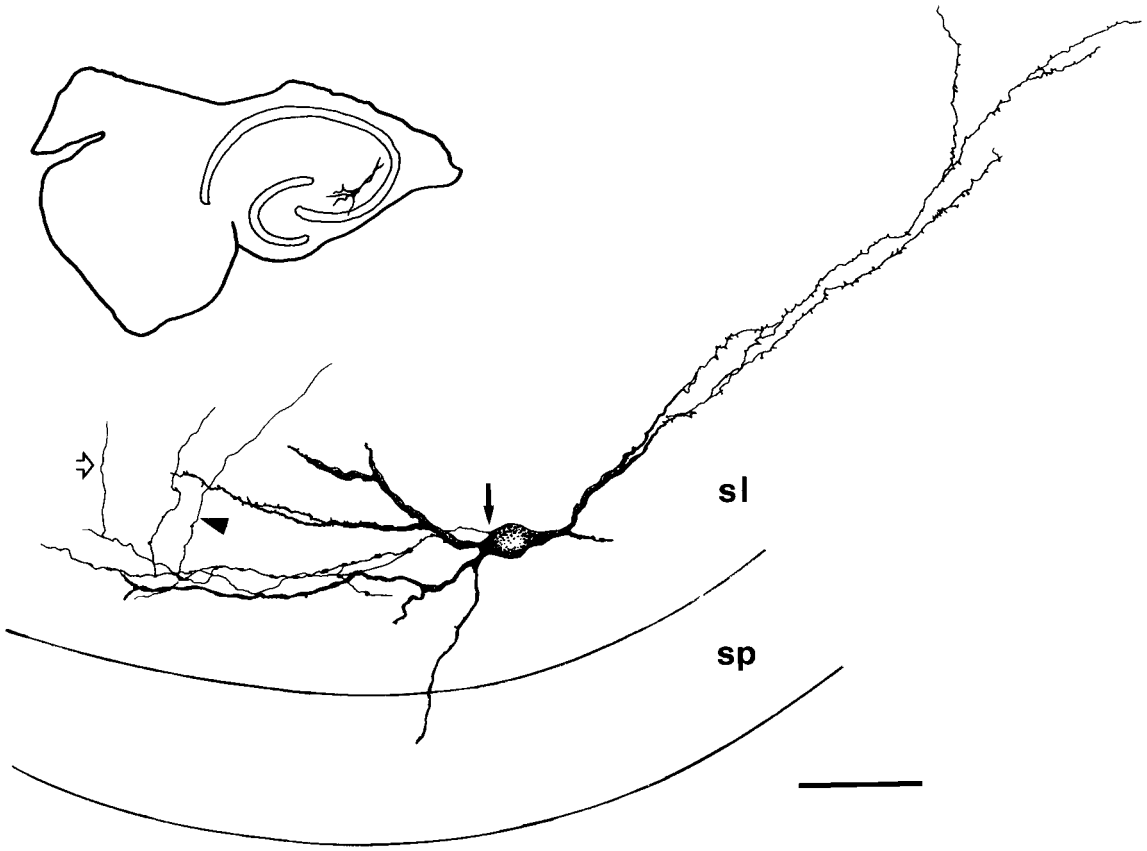

Fig. 2. Camera lucida drawing of a spiny stratum lucidum neuron subjected to correlated light and electron microscopic analysis. Inset shows the position of the neuron in the slice. The arrow indicates the origin of the axon from the soma. The arrowhead indicates the axon collateral shown in Figure 3B. An open arrow marks the ascending axonal collateral shown in Figure 4A. Note the numerous, occasionally very long, spines on the dendrites. sl, stratum lucidum; sp, stratum pyramidale. Scale bar = 100 μm.

approximately perpendicular to the dendritic axis of CA3 pyramidal neurons. The spiny neurons observed in stratum lucidum are likely to be the same neurons as those recently described for the first time in this region using an antibody against the calcium-binding protein calretinin (Gulyás et al., 1992) and in Golgi studies (Soriano and Frotscher, 1993a). The dendritic arborization of the neurons observed here is similar to that described in these previous studies of spiny stratum lucidum neurons: the majority of the dendrites remain in the stratum lucidum, some dendrites extend into stratum radiatum but not into stratum lacunosum–moleculare, others into stratum pyramidale; very rarely were dendrites observed in stratum oriens (Figs. 1A,B, 2, 3A, 5A).

Figure 2 shows a camera lucida drawing, and Figure 3 photomicrographs of a typical spiny neuron in stratum lucidum with dendritic spines illustrated at higher magnification (Fig. 3B–E). The spines were generally long and thin. Specialized, highly branching spines, like the thorny excrescences found in stratum lucidum on CA3 pyramidal neurons (Hamlyn, 1962; Blackstad and Kjaerheim, 1961), were never observed on these neurons. The relatively low number of spines observed in the spiny cells of our material may be due to the young age of the animals used in the present study (see also Discussion).

Synaptic contacts onto spiny neurons

Despite the absence of thorny excrescences, it is likely that these neurons receive synaptic inputs from mossy fibers, because the majority of their dendrites were located in the stratum lucidum. Electron microscopic examination of the spiny neuron shown in Figures 2 and 3 revealed that spiny neurons in stratum lucidum receive synaptic input from large terminals, most likely mossy fiber boutons (data not shown; see Gulyás et al., 1992, Soriano and Frotscher, 1993a). Contacts of mossy fiber boutons were observed on dendritic shafts and were identified by their large size and numerous synaptic vesicles, including the dense core vesicles characteristic of mossy fiber boutons (Blackstad and Kjaerheim, 1961; Hamlyn, 1962). In addition to these large boutons, however, other synaptic contacts from smaller presynaptic terminals were observed on both dendritic spines and on shafts. These synapses could originate from a number of possible sources, including smaller en passant mossy fiber boutons (Soriano and Frotscher, 1993a; Frotscher et al., 1994), recurrent collaterals of CA3 pyramidal neurons, local circuit inhibitory neurons, or longer range inputs to the hippocampus. In many cases, the long spines of the spiny stratum lucidum neurons were found to receive synaptic inputs from multiple synaptic terminals.

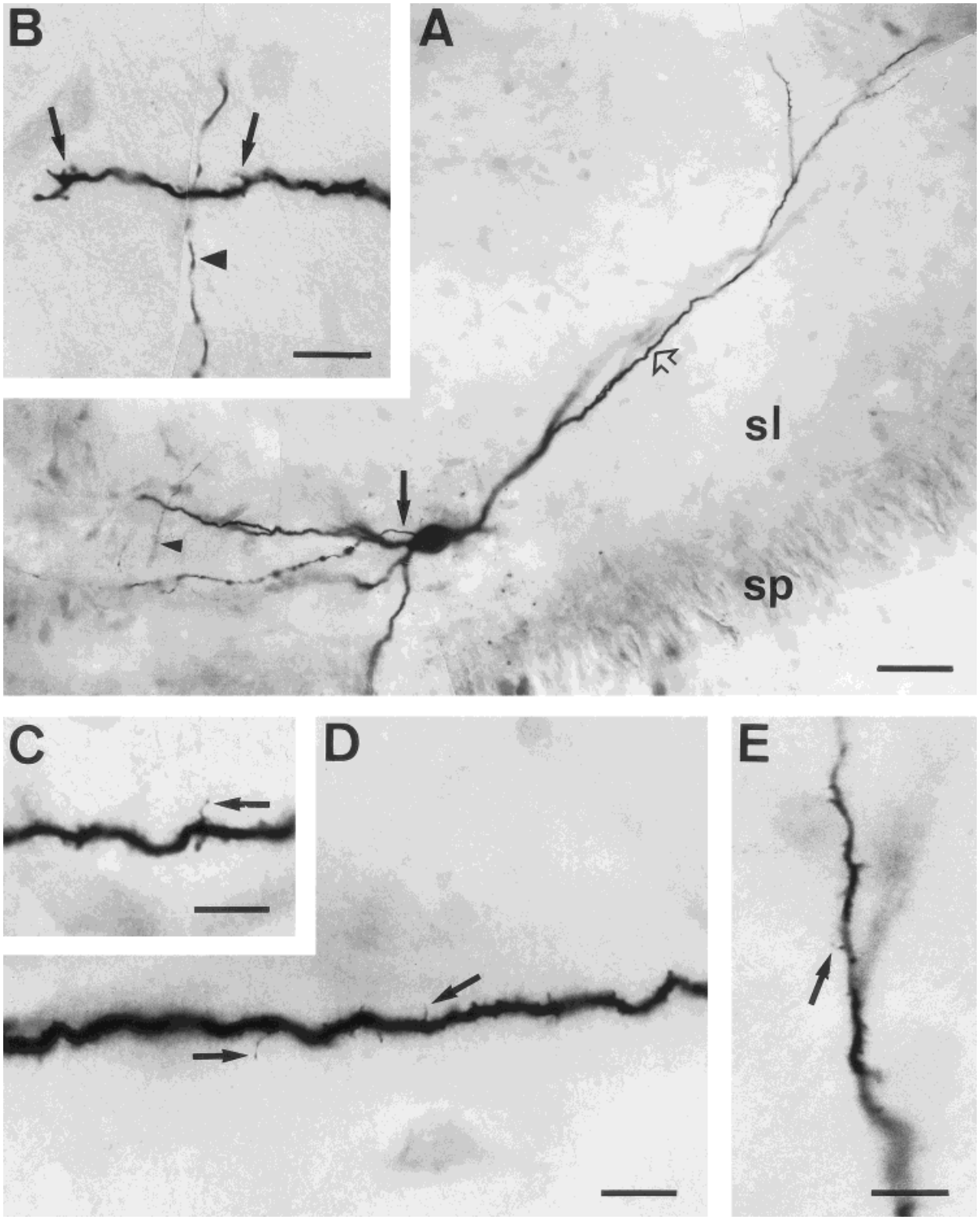

Fig. 3. Photomicrograph of the same spiny neuron shown in Figure 2. **A:** The arrow and arrowhead label the axon origin and the axonal collateral, respectively, shown in Figure 2. The open arrow indicates a dendritic segment shown at higher magnification in D. **B:** Dendritic segment crossed by an axonal collateral. The arrowhead corresponds to the same spot labeled in A by an arrowhead and in Figure 2. The arrows point to spines on the dendrite. **C–E:** Various dendritic segments of the cell illustrated in A. Arrows point to the thin, long spines. Scale bars = 50 μm in A, 20 μm in B, 10 μm in C–E.

Axonal projection of spiny neurons

The axons of spiny stratum lucidum neurons originated at the soma (Figs. 1B, 2, and 5A) or at a proximal dendrite (Fig. 1A) and had extensive collaterals. The majority of these collaterals remained within the stratum lucidum and stratum radiatum, but some collaterals extended into stratum lacunosum-moleculare, and a few traversed stratum pyramidale and entered stratum oriens (Fig. 1B). The vast majority of axon collaterals remained within the CA3 region, but in a small number of cases, axon collaterals were also observed extending into the stratum radiatum of CA1 and into the hilar region of the dentate gyrus.

Axons were never observed to enter the output pathways of the hippocampus such as the fimbria or the alveus. These neurons therefore appear to be largely local circuit neurons, but we cannot rule out that some longer range connections exist, as some collaterals could have been cut during slice preparation. For example, collaterals that projected longitudinally, as are known to exist in the case of mossy cells in the hilus (Amaral and Witter, 1994), would not be observed with our methods. It should be noted, however, that neurons with such projections have never been identified using retrograde labeling methods (Swanson et al., 1981), further supporting the idea that spiny neurons in stratum lucidum are local circuit neurons.

To determine whether local axon collaterals actually gave rise to synaptic contacts, an effort was made to follow some axonal collaterals in serial sections in the electron microscope. This process was made particularly difficult because the fine structural details of presynaptic terminals were often obscured by the electron-dense DAB reaction product. Nevertheless, a total of 15 synapses were identified with the electron microscope. An example of such a synapse, from an axonal collateral located in stratum lucidum (see Figs. 2, 4A), is shown in Fig. 4B,C. The confirmation of synaptic contacts arising from such local axon collaterals demonstrates that these neurons function at least partially as local circuit neurons.

Physiological properties of spiny neurons

The physiological properties determined for spiny neurons in stratum lucidum are given in Table 1, and an example of typical active and passive physiological responses is shown in Figure 5. The slow membrane time constant (τ_0) and input resistance (R_N) of the spiny stratum lucidum neurons, determined from small current steps near the resting potential, in physiological solution with no blockers of active conductances present, appeared most similar to that previously determined for granule cells of the dentate gyrus (Spruston and Johnston, 1992). τ_0 from the spiny stratum lucidum neurons was slower than that of CA1 pyramidal neurons and faster than that of CA3 pyramidal neurons (Table 1; Spruston and Johnston, 1992), suggesting that spiny neurons located in stratum lucidum have a membrane resistivity (R_m) intermediate to these two types of pyramidal neurons. The input resistance, R_N, however, was higher than that of both CA1 and CA3 pyramidal neurons, presumably due to the smaller somata and dendritic trees in these neurons compared with hippocampal pyramidal neurons.

The physiological properties of spiny neurons in stratum lucidum are quantitatively compared with CA3 pyramidal neurons under conditions identical to those used for recordings from stratum lucidum neurons (see Table 1). In addition to the differences in passive membrane properties mentioned above, spiny neurons in stratum lucidum appeared to have more depolarized resting potentials, fire faster, and have larger fast spike afterhyperpolarizations than the neighboring CA3 pyramidal neurons.

Dendritic arborizations of aspiny neurons

In addition to the spiny neurons described above, aspiny neurons with their cell bodies in stratum lucidum were also identified (Figs. 6A–C, 7A, 8A). The somata of these neurons were generally bipolar, giving rise to two to five primary dendrites that to a varying extent displayed varicose swellings in their course. Like the dendrites of the spiny neurons, these dendrites branched extensively in stratum lucidum and stratum radiatum of CA3; unlike the spiny neurons, however, some dendrites of aspiny neurons traversed stratum pyramidale and entered stratum oriens (Figs. 6B,C, 8A).

Axonal projection of aspiny neurons

The axons of aspiny stratum lucidum neurons usually originated at the soma (Fig. 6A,C), but in some cases they originated from a proximal primary dendrite (Fig. 6B). Two types of aspiny neurons were observed with respect to their axonal collaterals. The first type (n = 5) had axonal collaterals that were largely restricted to stratum lucidum and stratum radiatum of the CA3 region (Fig. 6A,C). In the second type (n = 11), the majority of axonal collaterals arborized in the stratum pyramidale and extended into stratum oriens of CA3 (Figs. 6B, 7A, 8A).

As was the case for the spiny neurons, no axon collaterals of aspiny neurons were observed to enter the fimbria or alveus, suggesting that they are local circuit neurons. Examples of local synaptic contacts identified with the electron microscope are shown in Figure 7B–D for a neuron with its terminal plexus in stratum pyramidale and stratum oriens of CA3 (Fig. 7A). These synapses were found on dendritic shafts (Fig. 7C) and cell bodies (Fig. 7B,D). The presynaptic boutons appeared larger than those of the spiny stratum lucidum cells. The target neurons may be CA3 pyramidal cells, but the existence of synapses on interneurons cannot be excluded without proper identification of the postsynaptic cell.

Physiological properties of aspiny neurons

Aspiny neurons in stratum lucidum had significantly faster maximal firing rates and shorter spike half widths than their spiny counterparts (Fig. 8). Despite these differences, there was substantial overlap of the ranges of these parameters in spiny and aspiny neurons, so these measures would not be reliable indicators of cell type in the absence of morphological analysis. The large range of many of the parameters indicated in Table 1 may reflect heterogeneity of the types of aspiny neurons in stratum lucidum. Analysis of the axon projection of these neurons suggests that two distinct populations of aspiny neurons might exist in stratum lucidum (see above), but our sample size was too small to determine whether these morphological differences correlated with physiological differences.

DISCUSSION

The stratum lucidum of the hippocampus is known to contain the densely packed bundle of mossy fibers, and one

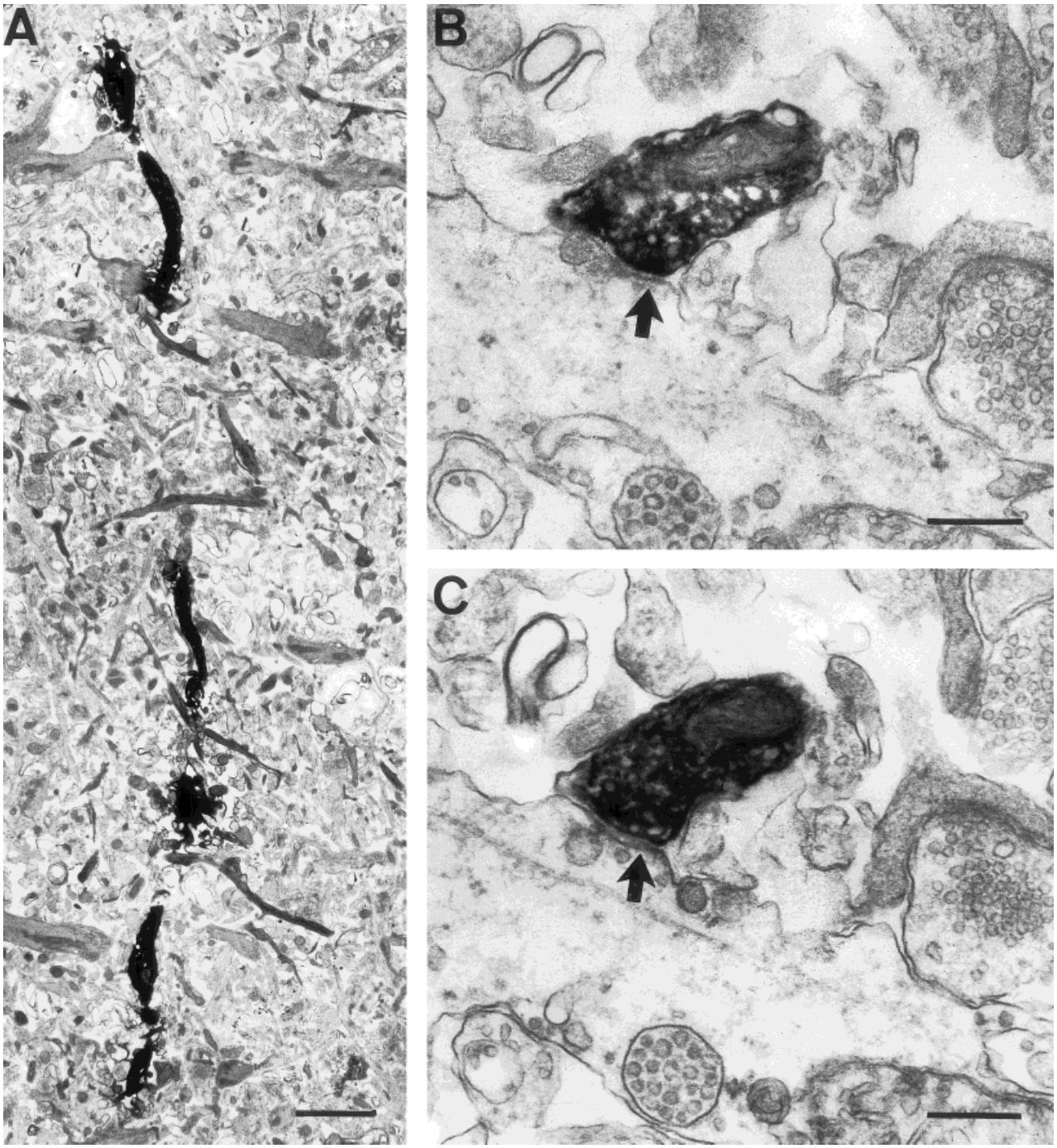

Fig. 4. Axonal collateral of a spiny neuron in stratum lucidum. **A:** Low-power electron micrograph of the axon collateral labeled by open arrow in Figure 2. **B,C:** Serial sections of a bouton, formed by the axon collateral shown in A. The arrows label a putative axodendritic synapse. Scale bars = 2 μm in A, 0.25 μm in B,C.

would not expect many cell bodies in this layer. Spiny neurons with their cell bodies located in stratum lucidum were first described by Gulyás et al. (1992) in immunocytochemical studies with an antibody against the calcium-binding protein calretinin and later in a Golgi study by Soriano and Frotscher (1993a). These cells constitute a class of hippocampal cells not described by either Ramón y Cajal (1911) or Lorente de Nó (1934). As the axonal projections could not be determined from either the Golgi impregnation or antibody staining methods by which the cells were discovered, we examined the axonal projection of these neurons using biocytin fills. In the course of this

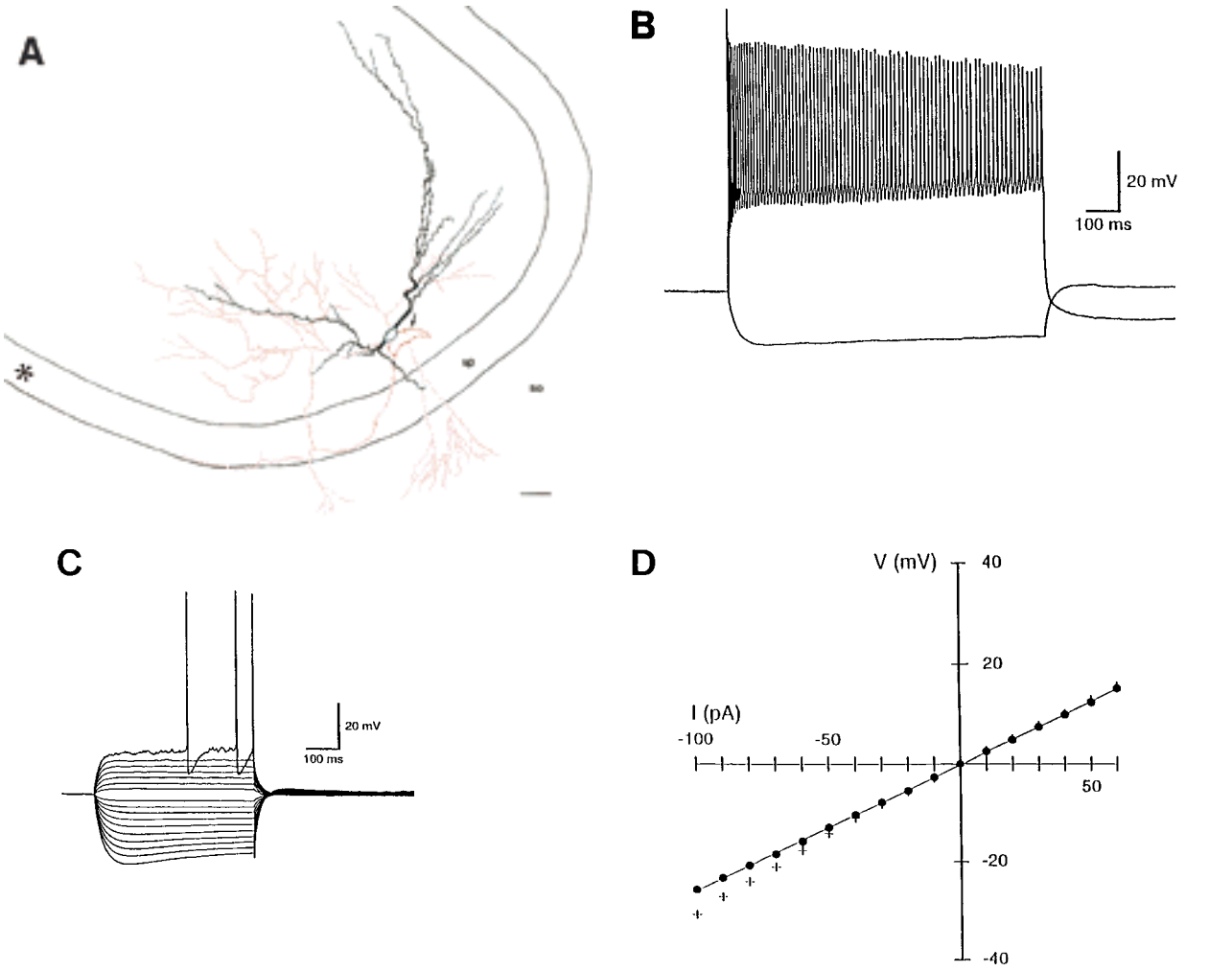

Fig. 5. Paired anatomy and physiology of a spiny neuron in stratum lucidum. **A:** Camera lucida drawing of the neuron whose physiology is shown in B–D; asterisk indicates CA3c. Arrow points to the origin of the axon. sp, stratum pyramidale; so, stratum oriens. **B:** Responses to 1-second current injections of +500 and -100 pA. Maximal firing (86 Hz) was observed with the +500 pA current injection. The hyperpolarizing response demonstrates some sag, with a steady-state to peak ratio of 0.83. **C:** Voltage responses to current injections of -100 to +60 pA, at 10 pA increments. τ_0 determined from the -40 and -20 to +20 pA pulses was 24 milliseconds. Action potential half-width was 0.88 milliseconds. **D:** Voltage-current relationship for the data shown in C. Steady-state voltages are indicated as filled circles and peak responses as crosses. The line shown is a linear regression through all the steady-state points. R_N, determined from the slope of this line, was 257 MΩ. Resting potential was -60 mV. Scale bar = 50 μm in A.

study we found a variety of cells of which only a few corresponded to the characteristic densely spiny neurons. Most cells had fewer spines than observed after Golgi impregnation or immunostaining for calretinin. The lower number of spines in our sample of neurons may be due to the developmental stage of the animals used in the present study or to some damage to these highly vulnerable cells (Hsu and Buzsáki, 1993) during slice preparation (see below). One might also argue then that the neurons which lack spines do not represent a separate group but an extreme form of a rather variable type of stratum lucidum neurons. We cannot exclude this possibility; however, there are a couple of arguments against this possibility: first, the dendritic orientation and the axonal distribution was somewhat different between spiny and aspiny stratum lucidum neurons, as were some of the physiological characteristics; second, dendrites of aspiny neurons often displayed varicosities that were absent in the spiny neurons; and third, the aspiny cells gave rise to larger presynaptic boutons than the spiny neurons. Therefore, we found the present classification useful in describing neuronal types in stratum lucidum. Analyzing the connectivity and physiology of these and other interneurons in the hippocampal formation (see Freund and Buzsáki, 1996 for review) is likely to be as important as analyzing the principal neurons for understanding the processes underlying spatial discrimination and learning and memory that occur in the hippocampal network.

Methodological considerations

Because the number of neurons with cell bodies in stratum lucidum is relatively small, recordings from these neurons in vivo and in vitro would be difficult without the benefit of visualization. Using infrared differential interference contrast videomicroscopy (Stuart et al., 1993), however, neurons in stratum lucidum were routinely patch

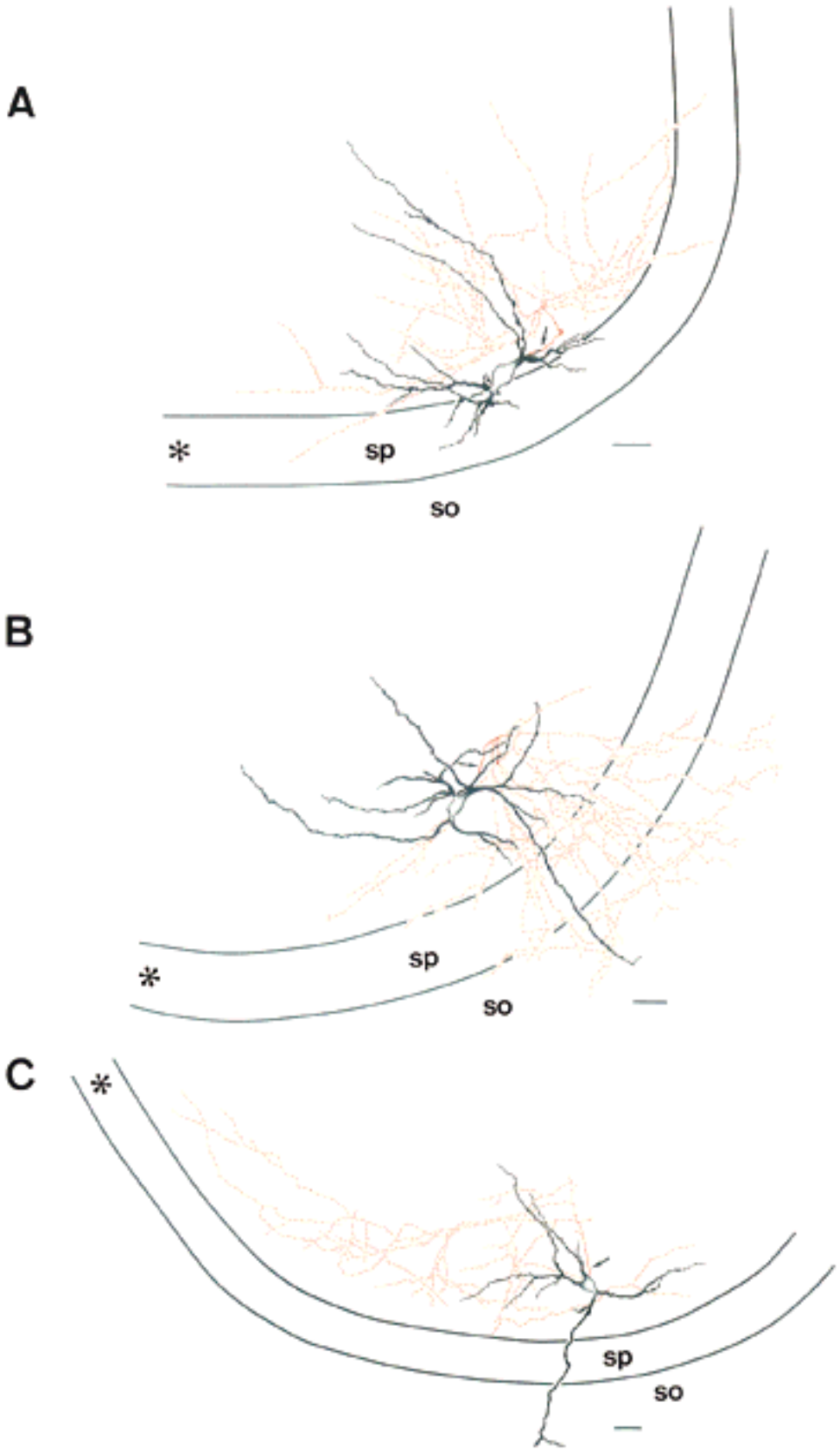

Fig. 6. Dendritic trees and axonal arborizations of three aspiny neurons in stratum lucidum **A–C:** This figure demonstrates the position of the cell bodies in stratum lucidum, the extent of the dendritic arborizations (black), and the extent of the axonal arborizations (red). Note that the axon collaterals in A and C are limited to the stratum lucidum and stratum radiatum, whereas the cell in B has axon collaterals mainly in stratum pyramidale and stratum oriens. The arrows indicate the origin of the axon. The asterisks indicate CA3c. sp, stratum pyramidale; so, stratum oriens. Scale bars = 50 μm.

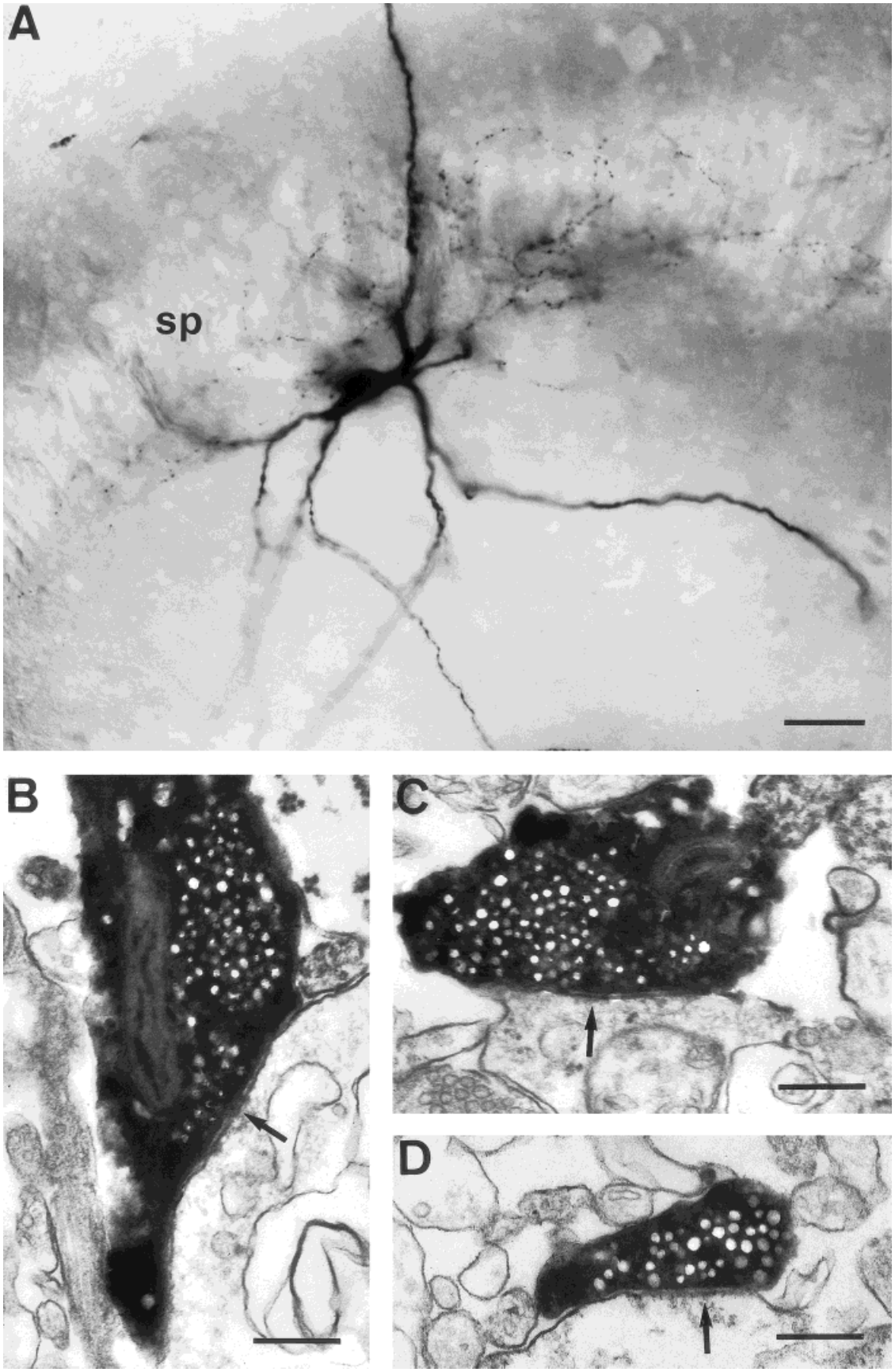

Fig. 7. **A:** Photomicrograph of an aspiny stratum lucidum cell with axon terminals in the stratum pyramidale (sp) (s.l. 013). B–D: Presynaptic terminals of an aspiny neuron in stratum lucidum. **B, D:** Contacts (arrows) on the cell body; **C:** contact (arrow) on a dendritic shaft. Scale bars = 50 µm in A, 0.25 µm in B–D.

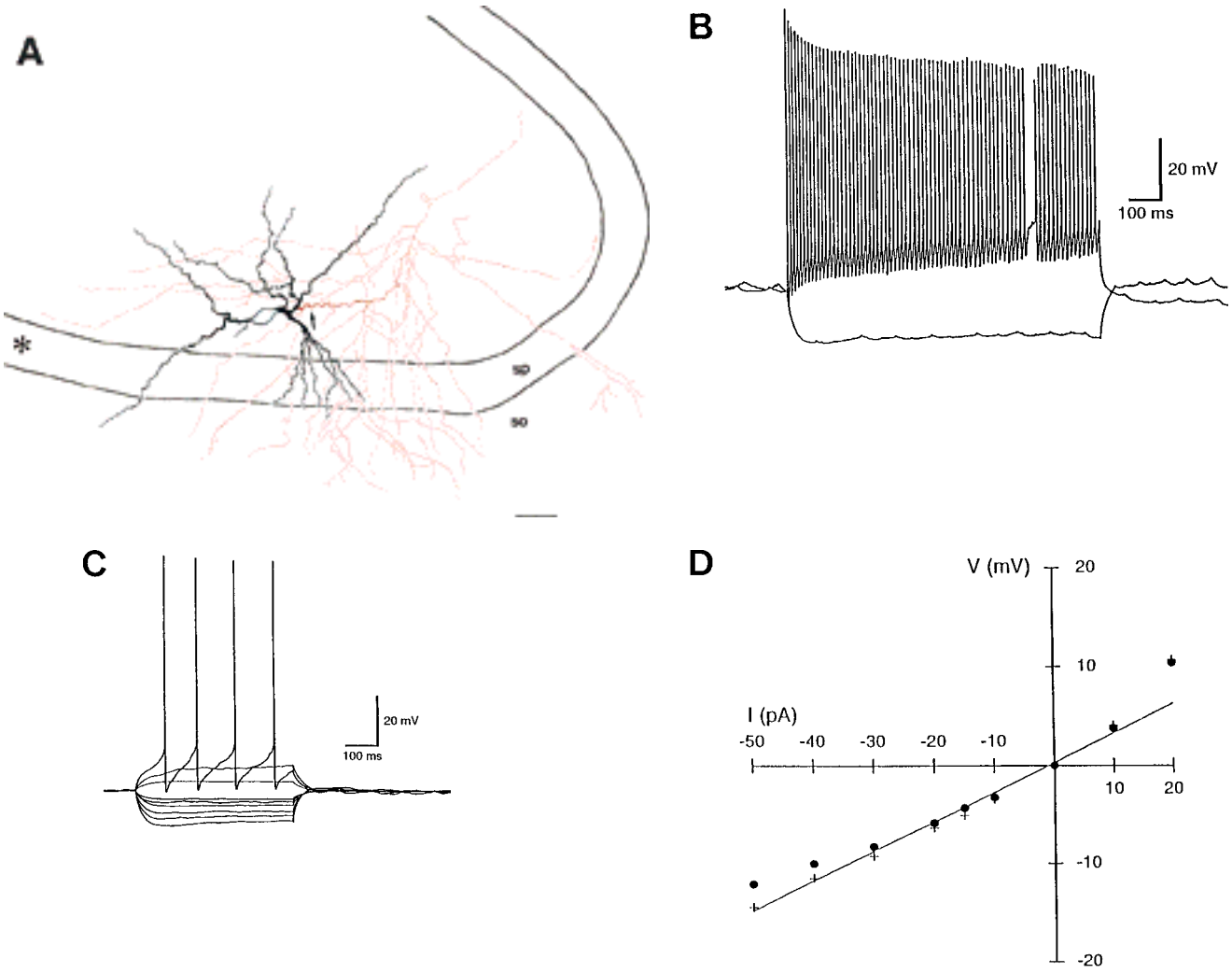

Fig. 8. Paired anatomy and physiology of an aspiny cell in stratum lucidum. **A:** Camera lucida drawing of the neuron whose physiology is shown in B–D; asterisk indicates CA3c. Arrow points to the origin of the axon. sp, stratum pyramidale; so, stratum oriens. **B:** Responses to 1-second current injections of +200 and -50 pA. Maximal firing (75 Hz) was observed with the +200 pA current injection. The hyperpolarizing response demonstrates some sag, with a steady-state to peak ratio of 0.83. **C:** Voltage responses to current injections of -50 to +20, at 10 pA increments. τ_0, determined from the -30 and -20 pulses, were 24 milliseconds. The action potential half-width was 0.54 milliseconds. **D:** The voltage-current relationship for the data shown in C. Steady-state voltages are indicated as filled circles, and peak responses as crosses. The line shown is a linear regression through the steady-state points between -30 and +10 pA. R_N, determined from the slope of this line, was 301 MΩ. Resting potential was -60 mV. Scale bar = 50 μm in A.

clamped in hippocampal slices. Along with its strengths, this approach has limitations. First, with the IR-DIC only neurons near the surface of the slice can be visualized, i.e., in a zone known to be more severely damaged during slice preparation than the central portion of the slice (Frotscher et al., 1981). As a result, the fine structural preservation is not optimal. Second, visualizing and recording from neurons in the stratum lucidum became progressively more difficult in slices that were prepared from older animals. We therefore used rats of age 13–28 days old. The results must therefore be interpreted with the caveat that both the anatomical and physiological properties of these neurons may undergo further postnatal development. This may hold true in particular for the density of spines. In adult animals a much larger number of spines on both cell bodies and dendrites of spiny stratum lucidum neurons were observed (Gulyás et al., 1992; Soriano and Frotscher, 1993a). Furthermore, it is well known that there is a spine loss after deafferentation (e.g. Parnavelas et al., 1974) that definitely occurs in slices. The spiny cells may be particularly vulnerable to ischemia (see below), and their degeneration may be accompanied by the loss of some spines. If so, we might have underestimated the abundance of spiny neurons in stratum lucidum.

Another problem is that use of slices limits analysis of the axonal projections to those maintained within the plane of the slice; longitudinal projections would not be observed. Although cut dendrites were occasionally observed, such damage did not appear to be extensive. However, axons may have a much wider distribution than dendrites, and we cannot exclude that these neurons have distant intrahippocampal or extrahippocampal targets.

The latter appears unlikely though, because we are not aware of any retrograde tracing study in which these cells were labeled after injection of the tracer into target regions of the hippocampus (Swanson et al., 1981). On the other hand, there is increasing evidence that many hippocampal neurons traditionally considered interneurons project to extrahippocampal regions, for instance to the septal complex (Alonso and Köhler, 1982; Tóth et al., 1993) and the nucleus accumbens (Hayes and Totterdell, 1985), or to the contralateral hippocampus (Ribak et al., 1986, Leranth and Frotscher, 1987; Deller et al., 1995). The issue may ultimately be solved by intracellular staining of these neurons in vivo.

Spiny stratum lucidum cells are involved in local circuits

We have shown here that the spiny stratum lucidum cells give rise to abundant axonal collaterals mainly in stratum lucidum and stratum radiatum of CA3, some of them reaching CA1 and the hilar region, respectively. Thus, even if these cells give rise to an extrahippocampal projection, they are preferentially involved in local circuits. Unfortunately, we were unable to classify the contacts formed by the collaterals of the stratum lucidum cells as symmetric or asymmetric synapses (Gray, 1959). Contacts exhibiting asymmetric membrane specializations are generally regarded as excitatory, and those with symmetric membrane specializations as inhibitory synapses. In a previous study, postembedding immunostaining of Golgi-impregnated and gold-toned spiny stratum lucidum cells revealed that these neurons were GABA-negative, but stained for glutamate, like adjacent CA3 pyramidal cells (Soriano and Frotscher, 1993a). It is difficult to infer the excitatory vs. inhibitory nature of the spiny stratum lucidum cells on the basis of their physiological properties. The slower maximal firing rate compared with the aspiny neurons might suggest an excitatory role, but this rate is significantly faster and the fast afterhyperpolarization significantly larger than in CA3 pyramidal neurons, suggesting that the spiny neurons might be inhibitory. In the absence of further, more conclusive data (e.g., immunostaining for glutamate decarboxylase and/or recordings from synaptically coupled pairs of neurons), assumptions as to the excitatory or inhibitory nature of these cell remain speculative. It should be mentioned, however, that recent physiological studies have provided evidence for excitatory interneurons in the CA3 region (Smith et al., 1995).

Previous studies have shown that the spiny stratum lucidum cells are heavily innervated by en passant synapses of preterminal mossy fiber axons and giant mossy fiber boutons (Gulyás et al., 1992; Soriano and Frotscher, 1993a). The mossy fibers may more efficiently drive these neurons than the CA3 pyramidal cells because the spiny stratum lucidum cells receive mossy fiber input not only on proximal dendrites (like the CA3 pyramidal cells) but also on more distal dendritic branches. The presence of a majority of the axon terminals in the stratum radiatum of CA3 suggests that these neurons give rise to a similar projection to stratum radiatum as the CA3 pyramidal cells, but with an emphasis on recurrent collaterals and a smaller feed-forward projection to CA1.

It has been speculated that the rapid degeneration of the spiny stratum lucidum cells under ischemic conditions is due to their massive innervation by mossy fibers and that this early loss of an important control mechanism in the CA3 region may cause the delayed degeneration of the CA1 pyramidal cells (Freund and Maglóczky, 1993; Hsu and Buzsáki, 1993). In this respect, the spiny stratum lucidum cells may be compared with the mossy cells of the hilar region (Hsu and Buzsáki, 1993), which, like the spiny stratum lucidum cells, are covered with spines (Amaral, 1978), receive mossy fiber input on both proximal and peripheral dendrites (Frotscher et al., 1994), contain calretinin (at least in mice, see Liu et al., 1996), and undergo rapid degeneration during ischemia (Hsu and Buzsáki, 1993).

Layer-specific termination of aspiny, putatively inhibitory stratum lucidum cells

The lack of spines and the formation of large synapses on cell bodies in the pyramidal cell layer of CA3 and on dendritic shafts in stratum radiatum and stratum oriens suggest that the aspiny stratum lucidum cells belong to the heterogeneous group of GABAergic inhibitory neurons. Aspiny neurons terminating in stratum lucidum and stratum radiatum probably synapse largely on the apical dendrites of CA3 pyramidal neurons, whereas those with their axons in stratum pyramidale and stratum oriens probably synapse on the somata and basal dendrites of CA3 pyramidal neurons. Pyramidal neurons are in fact the dominating cells in CA3; however, with the present approach it cannot be determined whether or not they are the only targets of these stratum lucidum cells. Recent studies have shown that some interneurons are specialized to control other interneurons in the rat hippocampus (Gulyàs et al., 1996). These two types of aspiny neurons in stratum lucidum probably constitute two functionally distinct populations of inhibitory interneurons. This probability is consistent with previous findings demonstrating a segregated, laminar organization of inhibitory interneuron terminations on CA1 pyramidal neurons and dentate granule cells (Halasy and Somogyi, 1993; Han et al., 1993; Soriano and Frotscher, 1993b; Frotscher et al., 1994; Buhl et al., 1994). The results presented here suggest that both of these aspiny cell types receive a dense input from the mossy fibers, as was shown before for other types of Golgi-impregnated or GABA-immunopositive, presumed inhibitory interneurons in the CA3 region (Frotscher, 1985; 1989). These aspiny neurons are therefore likely to be part of feed-forward or feedback inhibitory systems within CA3, controlling the excitatory impulse flow in regio inferior of the hippocampus.

ACKNOWLEDGMENTS

The authors thank Drs. Peter Jonas and Tamàs F. Freund for critically reading the manuscript. We are grateful to Sigrun Nestel, Barbara Joch, and Marianne Winter for technical assistance. This work was supported by the Alexander von Humboldt Foundation (N.S.), the "von Helmholtz-Programm" of the BMBF (J.L.), and the Deutsche Forschungsgemeinschaft Fr 620/1-6 and Leibniz Programm (M.F.).

LITERATURE CITED

Amaral, D.G. (1978) A Golgi study of cell types in the hilar region of the hippocampus of the rat. J. Comp. Neurol. *182*:851–914.

Amaral, D.G. (1993) Emerging principles of intrinsic hippocampal organization. Curr. Opin. Neurobiol. *3:*225–229.

Amaral, D.G., and M. P. Witter (1994) The hippocampal formation. In G. Paxinos (ed): The Rat Nervous System, 2nd Ed. New York: Academic Press.

Alonso, A., and C. Köhler (1982) Evidence of separate projections of hippocampal pyramidal and non-pyramidal neurons to different parts of the septum in the rat brain. Neurosci. Lett. *31:*209–214.

Berger, T.W., G. Chauvet, and R.J. Sclabassi (1994) A biologically based model of the functional properties of the hippocampus. Neural Networks *7:*1031–1064.

Blackstad, T.W., and A. Kjaerheim (1961) Special axodendritic synapses in the hippocampal cortex: Electron and light microscopic studies on the layer of mossy fibers. J. Comp. Neurol. *117:*113–159.

Buhl, E.H., K. Halasy, and P. Somogyi (1994) Diverse sources of hippocampal unitary inhibitory postsynaptic potentials and the number of synaptic release sites. Nature *368:*823–828.

Deller, T., R. Nitsch, and M. Frotscher (1995) Phaseolus vulgaris-leucoagglutinin tracing of commissural fibers to the rat dentate gyrus: Evidence for a previously unknown commissural projection to the outer molecular layer. J. Comp. Neurol. *325:*55–68.

Freund, T.F., and Buzsáki, G. (1996) Interneurons of the hippocampus. Hippocampus *6*:345– 470.

Freund, T.F., and Z. Maglòczky (1993) Early degeneration of calretinin-containing neurons in the rat hippocampus after ischemia. Neuroscience *56*:581–596.

Fricke, R.A., and D.A. Prince (1984) Electrophysiology of dentate gyrus granule cells. J. Neurophysiol. *51:*195–209.

Frotscher, M., U. Misgeld, and C. Nitsch (1981) Ultrastructure of mossy fibre endings in *in vitro* hippocampal slices. Exp. Brain. Res. *41:*247–255.

Frotscher, M. (1985) Mossy fibres form synapses with identified pyramidal basket cells in the CA3 region of the guinea pig hippocampus: A combined Golgi-electron microscope study. J. Neurocytol. *14:*245–259.

Frotscher, M. (1988) Neuronal elements in the hippocampus and their synaptic connections. In: Frotscher M, Kugler P, Misgeld U, Zilles K: Neurotransmission in the hippocampus. Adv. Anat. Embryol. Cell Biol. *111:*2–19.

Frotscher, M. (1989) Mossy fiber synapses on glutamate decarboxylase-immunoreactive neurons: Evidence for feed-forward inhibition in the CA3 region of the hippocampus. Exp. Brain Res. *75:*441–445.

Frotscher, M., E. Soriano, and U. Misgeld (1994) Divergence of hippocampal mossy fibers. Synapse *16:*148–160.

Gray, E.G. (1959) Axo-somatic and axo-dendritic synapses of the cerebral cortex. J. Anat. (Lond) *93:*420–433.

Gulyás, A.I., R. Miettinen, D.M. Jacobowitz, and T.F. Freund (1992) Calretinin is present in non-pyramidal cells of the rat hippocampus. I. A new type of neuron specifically associated with the mossy fibre system. Neuroscience *48:*1–27.

Gulyás, A.I., N. Hájos, and T.F. Freund (1996) Interneurons containing calretinin are specialized to control other interneurons in the rat hippocampus. J. Neurosci. *16:*3397–3411.

Halasy, K., and P. Somogyi (1993) Subdivisions in the multiple GABAergic innervation of granule cells in the dentate gyrus of the rat hippocampus. Eur. J. Neurosci. *4:*144–153.

Hamlyn, L.H. (1962) The fine structure of mossy fibre endings in the hippocampus of the rabbit. J. Anat. *97:*112–120.

Han, Z.-S., E.H. Buhl, Z. Lörinczi, and P. Somogyi (1993) A high degree of spatial selectivity in the axonal and dendritic domains of physiologically identified local-circuit neurons in the dentate gyrus of the rat hippocampus. Eur. J. Neurosci. *5*:395–410.

Hayes, L., and S. Todderdell (1985) A light and electron microscopic study of non-pyramidal hippocampal cells that project to the medial nucleus accumbens. Neurosci. Lett. *22(Suppl.):* 507.

Hsu, M., and G. Buzsáki (1993) Vulnerability of mossy fiber targets in the rat hippocampus to forebrain ischemia. J. Neurosci. *13:*3964–3979.

Leranth, C., and M. Frotscher (1987) Cholinergic innervation of hippocampal GAD- and somatostatin-immunoreactive commissural neurons. J. Comp. Neurol. *261:*33–47.

Liu, Y., N. Fusije, and T. Kosaka (1996) Distribution of calretinin immunoreactivity in the mouse dentate gyrus. I. General description. Exp. Brain Res. *108:*389–403.

Lorente de Nó, R. (1934) Studies on the structure of the cerebral cortex. II. Continuation of the study of the Ammonic system. J. Psychol. Neurol. *46:*113–177.

Madison, D.V., and R.A. Nicoll (1984) Control of the repetitive discharge of rat CA1 pyramidal neurones in vitro. J. Physiol. (Lond.) *354:*319–331.

Misgeld, U., and M. Frotscher (1986) Postsynaptic-GABAergic inhibition of non-pyramidal neurons in the guinea pig hippocampus. Neuroscience *19:*193–206.

Parnavelas, J.G., G. Lynch, N. Brecha, C.W. Cotman, and A. Globus (1974) Spine loss and regrowth in the hippocampus following deafferentiation. Nature *248:*71–73.

Purpura, D.P., S. Prelevic, and M. Santini (1968) Hyperpolarizing increase in membrane conductance in hippocampal neurons. Brain. Res. *7:*310–312.

Ramón y Cajal, S. (1911) Histologie du Système Nerveux de L'homme et des Vertébrés. Bd. I, Paris: Maloine.

Ribak, C.E., L. Seress, G.M. Peterson, K.B. Seroogy, J.H. Fallon, and L.C. Schmued (1986) A GABAergic inhibitory component within the hippocampal commissural pathway. J. Neurosci. *6:*3492–3498.

Scharfman, H.E. (1992) Differentiation of rat dentate neurons by morphology and electrophysiology in hippocampal slices: Granule cells, spiny hilar cells and aspiny 'fast spiking' cells. In C.E. Ribak, C.M. Gall, and I. Mody, (eds): The Dentate Gyrus and its Role in Seizures. New York: Elsevier, pp. 93–109.

Smith, K.L., D.H. Szarowski, J.N. Turner, and J.W. Swann (1995) Diverse neuronal populations mediate local circuit excitation in area CA3 of developing hippocampus. J. Neurophysiol. *74:*650–672.

Soriano, E., and M. Frotscher (1993a) Spiny nonpyramidal neurons in the CA3 region of the rat hippocampus are glutamate-like immunoreactive and receive convergent mossy fiber input. J. Comp. Neurol. *332:*435–448.

Soriano, E., and M. Frotscher (1993b) GABAergic innervation of the rat fascia dentata: A novel type of interneuron in the granule cell layer with extensive axonal arborization in the molecular layer. J. Comp. Neurol. *334:*385–396.

Spigelman, I., L. Zhang, and P.L. Carlen (1992) Patch-clamp study of postnatal development of CA1 neurons in the rat hippocampal slices: Membrane excitability and K^+ currents. J. Neurophysiol. *68:*55–69.

Spruston, N., and D. Johnston (1992) Perforated patch-clamp analysis of the passive membrane properties of three classes of hippocampal neurons. J. Neurophysiol.*67:*508–529.

Staley, K.J., T.S. Otis, and I. Mody (1992) Membrane properties of dentate gyrus granule cells: Comparison of sharp microelectrode and whole cell recordings. J. Neurophysiol. *67:*1346–1358.

Stuart, G., H.-U. Dodt, and B. Sakmann (1993) Patch-clamp recordings from the soma and dendrites of neurons in brain slices using infrared video microscopy. Pflügers Arch. *423:*511–518.

Storm, J.F. (1987) Action potential repolarization and a fast after-hyperpolarization in rat hippocampal pyramidal cells. J. Physiol. (Lond.) *385:*733–759.

Swanson, L.W., P.E. Sawchenko, and W.M. Cowan (1981) Evidence for collateral projections by neurons in Ammon's horn, the dentate gyrus, and the subiculum: A multiple retrograde labeling study in the rat. J. Neurosci. *1:*548–559.

Tóth, K., Z. Borhegyi, and T. F. Freund (1993) Postsynaptic targets of GABAergic hippocampal neurons in the medial septum-diagonal band of Broca complex. J. Neurosci. *13:*3712–3724.

Treves, A., and E.T. Rolls (1994) A computational analysis of the role of the hippocampus in memory. Hippocampus *4:*374–391.

Wilson, M.A., and B.L. McNaughton (1993) Dynamics of the hippocampal ensemble code for space. Science *261:*1055–1058.

Zola-Morgan, S., and L.R. Squire (1993) Neuroanatomy of memory. Annu. Rev. Neurosci. *16:*547–563.